MAS NMR structure refinement of uniformly 13C enriched chlorophyll a/water aggregates with 2D dipolar correlation spectroscopy

Boender, G.J.; Raap, J.; Prytulla, S.; Oschkinat, H.; Groot, H.J.M. de

MAS NMR structure refinement of uniformly ^{13}C enriched chlorophyll a/water aggregates with 2D dipolar correlation spectroscopy

G.J. Boender [a], J. Raap [a], S. Prytulla [b], H. Oschkinat [b], H.J.M. de Groot [a]

[a] *Leiden Institute of Chemistry, Gorlaeus Laboratories, Leiden University, P.O. Box 9502, 2300 RA Leiden, The Netherlands*
[b] *EMBL, P.O. Box 10.2209, D-69117 Heidelberg, Germany*

Abstract

2D MAS dipolar correlation spectroscopy of uniformly ^{13}C enriched chlorophyll a/water aggregates was performed using broadband RFDR to promote exchange of coherence through homonuclear dipolar couplings. It is shown experimentally that incorporation of TPPI and coherence pathway selection in the RFDR pulse scheme yields virtually pure 2D absorption lineshapes. From a series of 2D correlation spectra collected at two spinning speeds with different mixing times of ~ 1 and ~ 10 ms all ^{13}C resonances of the chlorophyll a molecule were assigned. The spectra with the longer mixing times reveal through-space intermolecular polarization transfer. This demonstrates that structural information can be obtained from uniformly ^{13}C enriched samples, which paves the way for a full structural characterization of amorphous solids.

1. Introduction

Chlorophyll a (Chl a) is the ubiquitous chromophore involved in light-harvesting and photochemistry in the photosynthetic energy conversion processes of green plants and related organisms. The chemical structure is depicted in Fig. 1. It consists of a macroaromatic cycle containing four pyrrole nitrogens coordinating a central Mg ion. When exposed to H_2O, Chl a can aggregate. It is thought that in the aggregated species water molecules form intermolecular hydrogen-bonded bridges from the Mg, with the water oxygen as a ligand, to the carbonyls 13^1, 13^3 and 17^3 [1,2].

Correlation spectroscopy of abundant nuclei is an important tool for structural characterization of biomolecules in solution [3,4]. Recently, important

progress towards general approaches for ^{13}C magic angle spinning (MAS) NMR 2D dipolar correlation spectroscopy in uniformly enriched small molecules using homonuclear dipolar interactions was reported [5–7]. For uniformly ^{13}C enriched solid-type samples MAS conditions are required for sufficiently high resolution. Through mixing with rotor-synchronized phase alternating trains of π pulses [8], the homonuclear dipolar interactions between the nuclei that are normally averaged by MAS can be partially restored, generating pathways for transfer of coherence between nearby nuclei in uniformly enriched materials [9,10].

In the present study we report considerable improvement of the resolution of the MAS radio-frequency-driven dipolar recoupling (RFDR) 2D correlation spectroscopy by applying time proportional

phase incrementation (TPPI). In addition, coherence pathway selection through phase cycling [11,12], was used to obtain virtually pure phase type 2D correlation spectra. It is shown that the resolution of the experiment is sufficient to obtain a large number of dipolar correlations, allowing the complete assignment of ^{13}C resonances. This is another step towards setting the stage for structure determination in microscopically ordered solids that are not accessible to diffraction methods.

2. Results and discussion

The ^{13}C cross-polarisation (CP) MAS NMR spectrum of the [U-^{13}C]Chl a/water aggregate is shown in Fig. 1. These data, collected with a spinning speed $\omega_r/2\pi = 13.00$ kHz, match well the results of Brown et al. [13] who performed MAS NMR investigations of the natural abundance species. Despite the uniform enrichment with ^{13}C, the MAS signal constitutes relatively narrow lines, reflecting the high degree of microscopic order in this aggregate. The linewidths of the ^{13}C enriched form are ≈ 2 ppm, approximately twice the linewidths of the natural abundance form, due to the presence of scalar and residual couplings.

The Chl a/water aggregate is well suited for an investigation with ^{13}C dipolar correlation methods.

The chemical shift dispersion, almost 200 ppm, is conveniently large and there are only a few protons attached to the macroaromatic ring. Therefore, heteronuclear decoupling is easily achieved for the ring carbons. In addition, short intermolecular C–C distances can be expected for stacked Chl a.

In an attempt to obtain pure-phase ^{13}C dipolar correlation spectra we have performed MAS NMR 2D correlation spectroscopy of [U-^{13}C]Chl a/water aggregates using the pulse sequence of Fig. 2. The phase of the entire variable amplitude [1]H–[13]C CP preparation prior to the evolution period t_1 was varied in a TPPI scheme [11]. Following Bennett et al. [5], an integral multiple n of XY-8 phase alternated rotor-synchronized trains of π pulses was used to promote exchange of coherence through dipolar interactions during the mixing period $\tau_m = 8n\tau_r$. The effect of such π-pulse trains on a nuclear spin $I = 1/2$ coupled to another spin $S = 1/2$ has been described in terms of average Hamiltonian theory, Floquet theory and a geometrical approach involving fictitious spin $1/2$ operators [5,7,9,10]. It appears that the mixing partially cancels the MAS averaging of the dipolar interaction while refocusing the chemical shift. For instance, in the average Hamiltonian approximation $\hat{\mathcal{H}}_m = \bar{d}_{IS}(\hat{I}_x\hat{S}_x + \hat{I}_y\hat{S}_y)$ remains for the evolution of the coherence during the mixing period [5,7]. The $\bar{d}_{IS} \propto r_{IS}^{-3}$ and contains in addition the necessary information regarding the Euler angles,
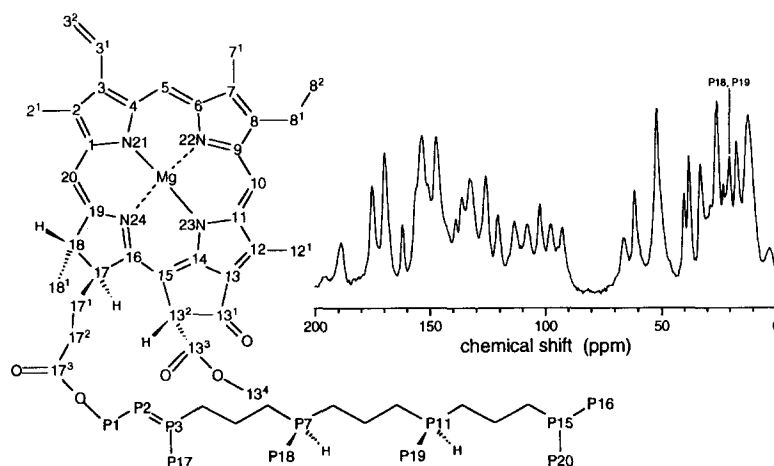

Fig. 1. Chemical structure of Chl a with the IUPAC numbering scheme and proton-decoupled ^{13}C CP/MAS spectrum of [U-^{13}C]Chl a/water aggregates. The tag indicates the P18, P19 resonances used for calibration of the chemical shift scale.

the chemical shift difference and the dependence on ω_r [5]. With a phase setting $\varphi_1 = 0$ the density operator at the end of the evolution time t_1 is

$$\hat{\rho}_e = -\hat{I}_y \cos(\omega_I t_1) - \hat{I}_x \sin(\omega_I t_1), \quad (1)$$

with ω_I the precession frequency of spin I.

During the mixing time τ_m the density operator is subject to $\hat{\mathcal{H}}_m$, yielding

$$\hat{\rho}_d = \left[-\hat{I}_y \cos^2\left(\tfrac{1}{2}\bar{d}_{IS}\tau_m\right) - \hat{S}_y \sin^2\left(\tfrac{1}{2}\bar{d}_{IS}\tau_m\right) \right.$$
$$\left. + \tfrac{1}{2}\left(\hat{I}_z\hat{S}_x - \hat{I}_x\hat{S}_z\right)\sin\left(\bar{d}_{IS}\tau_m\right) \right] \cos(\omega_1 t_1)$$
$$+ \left[-\hat{I}_x \cos\left(\tfrac{1}{2}\bar{d}_{IS}\tau_m\right) + \hat{I}_y\hat{S}_z \sin\left(\tfrac{1}{2}\bar{d}_{IS}\tau_m\right) \right]$$
$$\times \sin(\omega_1 t_1) \quad (2)$$

at the start of detection time t_2, in the case of $\varphi_2 = \varphi_3 = 0$. In addition to the desired polarisation transfer between $\hat{I}_y$ and $\hat{S}_y$, this density operator contains the transverse coherence $\hat{I}_x \cos(\tfrac{1}{2}\bar{d}_{IS}\tau_m)$, yielding dispersive components in the 2D RFDR spectrum. During detection, both the $(\hat{I}_z\hat{S}_x - \hat{I}_x\hat{S}_z)\sin(\bar{d}_{IS}\tau_m)$ and the $\hat{I}_y\hat{S}_z \sin(\tfrac{1}{2}\bar{d}_{IS}\tau_m)$ terms do not lead to observable magnetization, if the two-spin system is not on a rotational resonance condition.

Table 1
8-step phase cycle used for the absorption mode dipolar correlation spectra. Phase angles correspond with those depicted in Fig. 2. $\varphi_1 =$ TPPI, where TPPI cycles the phase of the entire preparation period with incrementing t_1 through 0, $\pi/2$, π and $3\pi/2$. φ_2 is used for ringdown elimination while φ_3 and φ_{ref} are used to select $0 \to \pm 1 \to 0 \to -1$ coherence transfer

	1	2	3	4	5	6	7	8
φ_2	0	0	0	0	π	π	π	π
φ_3	0	$\pi/2$	π	$3\pi/2$	0	$\pi/2$	π	$3\pi/2$
φ_{ref}	0	$\pi/2$	π	$3\pi/2$	π	$3\pi/2$	0	$\pi/2$

The two-spin average Hamiltonian approximation does not take into account that higher order coherences involving three or more spins may develop during mixing, in particular for highly uniformly enriched systems where the high level of enrichment facilitates an increase in the order of coherence upon
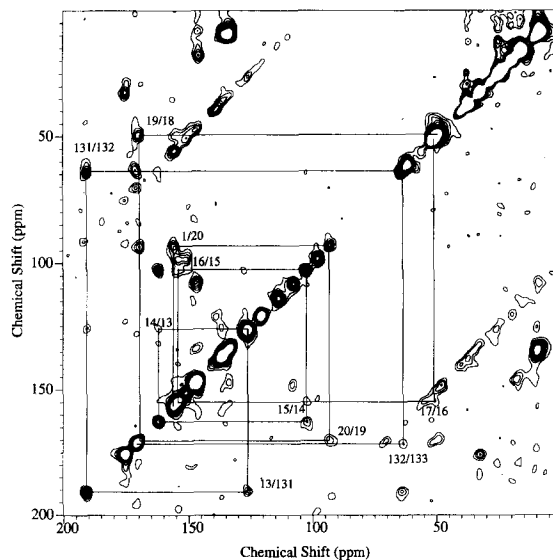
Fig. 3. Contour plot of an absorption mode MAS 2D ^{13}C dipolar correlation spectrum of [U-^{13}C]Chl a/water aggregates collected with the pulse sequence of Fig. 2 at a spinning speed $\omega_r/2\pi = 10000 \pm 5$ Hz with $n = 1$ yielding $\tau_m = 800 \pm 1$ μs. The FIDs were recorded with $2k$ data points and the same amount was used for zero filling. 256 points in the t_1 dimension were recorded. In the t_2 dimension a Lorentz–Gauss transformation with a narrowing of 50 Hz and a broadening of 150 Hz was applied prior to Fourier transformation. The horizontal and vertical lines indicate sequences of nearest-neighbour correlations. The assignments of correlations (x/y) on the plot correspond with the scheme in Fig. 1.
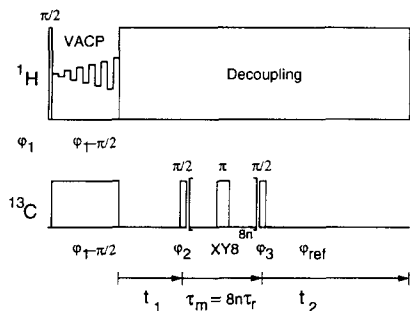

Fig. 2. Schematic representation of the phase-sensitive RFDR pulse sequence used for the absorption mode 2D MAS dipolar correlation experiments. Relevant rotation angles are depicted on top of the corresponding pulse, while the rf phases are indicated beneath the pulses. The entire [1]H–[13]C VACP preparation phase φ_1 was varied in a TPPI scheme. An XY-8 train of rotor-synchronized π pulses during the mixing time $\tau_m = 8n\tau_r$ with phases $(XYXYYXYX)_n$ was applied to favour transfer of coherence through homonuclear ^{13}C dipolar couplings. Coherence transfer pathway selection and ringdown elimination was attained with a phase cycle for φ_2, φ_3 and φ_{ref} listed in Table 1. t_1 and t_2 indicate evolution and acquisition times according to standard conventions.

Table 2

^{13}C chemical shifts (ppm) of Chl **a** in [U-^{2}H]tetrahydrofuran and in the aggregated form. Solution shifts (σ_{liq}) were taken from Ref. [15]. The σ_i are the isotropic shifts in the aggregated form with the estimated errors in parentheses. The numbering is according to the scheme in Fig. 1

No.	σ_{liq}	σ_i
12[1]	12.6	8.9 (0.3)
2[1]	12.6	9.6 (0.3)
7[1]	11.2	10.5 (0.3)
p17	16.2	16.8 (0.3)
8[2]	18.0	17.8 (0.2)
8[1]	20.0	20.2 (0.3)
p18	20.0	20.0 (0.2)
p19	20.0	20.0 (0.2)
p20	23.0	23.1 (0.2)
p16	23.0	23.1 (0.2)
18[1]	23.9	25.9 (0.6)
p9	25.2	25.5 (0.4)
p13	25.6	25.5 (0.4)
p5	25.8	25.5 (0.4)
p15	28.7	28.5 (0.2)
17[2]/17[1] [a]	30.1/30.9	32.5 (0.5)
p7	33.4	33.3 (0.3)
p11	33.6	33.3 (0.3)
p6	37.4	37.4 (0.2)
p12	38.0	37.9 (0.2)
p8	38.0	37.9 (0.2)
p10	38.0	37.9 (0.2)
p14	40.1	40.1 (0.2)
p4	40.4	40.4 (0.2)
18	50.0	50.0 (0.2)
17	51.6	51.4 (0.3)
13[4]	52.0	52.0 (0.2)
p1	61.3	61.5 (0.4)
13[2]	66.2	64 (1)
20	92.8	93.3 (0.4)
5	100.0	98.1 (0.4)
15	106.2	102.8 (0.4)
10	107.1	108.2 (0.4)
3[2]	118.9	113.4 (0.3)
p2	119.4	120.7 (0.2)
13/3[1] [a]	131.5	126.2 (0.3)
7	134.0	133.4 (0.4)
12	134.2	134.0 (0.4)
2	135.5	136.1 (0.2)
3	139.0	137.0 (0.2)
p3	142.2	139.0 (0.2)
8	144.1	146.2 (0.2)
9/11 [a]	146.1/147.7	147.2 (0.4)
4	148.0	150.7 (0.4)
6	151.4	154.4 (0.4)
16	155.8	154.0 (0.4)

Table 2 (continued)

No.	σ_{liq}	σ_i
1	154.0	155.9 (0.4)
14	161.4	162.0 (0.2)
19	167.4	170.0 (0.2)
13[3]	171.0	171.2 (0.4)
17[3]	172.7	175.3 (0.2)
13[1]	189.3	190.6 (0.2)

[a] The differences between C-9, C-11 and C-17[2], C-17[1] could not be resolved due to ambiguities in the intramolecular correlation pattern. The separation of 13 and 3[1] is not conclusive because of the occurrence of intermolecular correlations.

application of a pulse train. The necessary selection of $p = 0 \rightarrow \pm 1 \rightarrow -1$ coherence transfer pathways while eliminating higher orders up to order $p = 3$ was achieved by cycling the phase of the $\pi/2$ pulse at the end of the longitudinal mixing period in conjunction with the receiver phase according to Table 1 [14]. Finally, probe ringdown elimination by spin temperature alternation was done by cycling the phase of the $\pi/2$ pulse at the start of the mixing period. This is essential to reduce baseline distortions. In addition, the direct carbon signal created by the detection pulse is also suppressed by alternating the φ_2 phase according to Table 1.

The utility of the absorption mode experiment is illustrated in Fig. 3, which shows an example of a 2D correlation spectrum of the aggregate, collected with an $\omega_r/2\pi = 10000 \pm 5$ Hz and $\tau_m = 800 \pm 1$ µs. In this spectrum the MAS sideband diagonals at $\pm \omega_r/2\pi$ are clearly visible as well as some strong 2D cross-peaks revealing transfer of coherence. Several of the cross-peaks and diagonal peaks are connected by horizontal and vertical lines illustrating how the molecular framework gives rise to a correlation network, similar to the assignment procedures in solution NMR. The high spinning speed used for the experiment in Fig. 3 minimizes the occurrence of rotational resonance effects, and of correlations between centerbands and sidebands of the same ^{13}C MAS pattern. In addition, the amplitudes of the sidebands of correlations are small when using high spinning speeds.

The 2D spectrum in Fig. 3 is not symmetric with

respect to the intensities of cross-peaks on opposite sides of the diagonal. Although some of the asymmetric signals are introduced by t_1-noise, we attribute the asymmetry primarily to differences in chemical shift anisotropy and CP efficiency. As a result the coherence transfer within a pair of spins in the 2D CP/MAS experiments should be intrinsically asymmetric.

The resolution of the set of 2D spectra is sufficient for identifying a large number of individual correlations arriving at a complete assignment of the ^{13}C resonances. An example is shown in Fig. 3 at a somewhat higher plot level. In Table 2 the solid state shifts obtained from the analysis of 2D correlation spectra collected at different spinning speeds $\omega_r/2\pi \approx 7$ and ≈ 10 kHz, with mixing times $\tau_m \approx 1$ and ≈ 10 ms, are compared with data for the molecule in solution [15]. The errors for the solid-state assignment are given in parentheses.

It appears that the atoms 2^1, 3^1 and 3^2, situated at one side of the Chl **a** molecule, and the atoms 13, 15 and 12^1 at the opposite side are shifted upfield by more than 3 ppm in the aggregate with respect to their chemical shifts in solution. For the two methyl groups 2^1 and 12^1 the upfield shift is most likely induced by the ring-current of the π system of the macroaromatic cycle of a neighbouring molecule [16]. For the 3^1 and 3^2 carbons, it is also possible that the upfield shifts are related to ring current effects. Such an interpretation would be in agreement with current models for the structure of the Chl **a**/water aggregates [1,17], in which the edges of the macrocycles of neighbouring molecules are above one another, and the atoms 2^1, 12^1, 3^1 and 3^2 are above the plane of a neighbouring molecule. On the other hand, it is unlikely that the upfield shifts of atoms 13 and 15 are due to ring currents, because in that case atoms 13^1, 14 and 13^2 should be shifted upfield by a similar amount. The shifts of carbons 13 and 15, in the rigid ring system, indicate that small negative charges of -0.03 electronic equivalent are stabilized on carbons 13 and 15 by the formation of the aggregate. Here we have used the empirical relation that a shift of $+160$ ppm corresponds with one elementary unit of positive charge for an aromatic or olefinic carbon [18].

The Chl **a**/water aggregate provides a typical example of a system where high-resolution solid

state ^{13}C NMR spectroscopy will be indispensable to providing information at the atomic level about the precise structure. Structural characterization of microscopically ordered biomolecular assemblies can, in principle, be achieved by MAS NMR methods using site-specific isotope labeling techniques and exploiting internuclear dipolar interactions. For instance, it has been shown that accurate distance information in large specifically enriched membrane proteins can be obtained using 1D or 2D MAS NMR spectroscopy [19–21]. However, any approach involving site-directed isotope labeling requires a fair estimate of the structure to begin with, since these NMR distance measurements are typically limited to a maximum of ≈ 6 Å between pairs of labels. In addition, the accuracy at the longer distances is not very good and many separate time-consuming labeling procedures and associated NMR experiments will be necessary to converge upon a full structure, even for a molecule such as Chl **a** with 55 carbon atoms, making this strategy a laborious experimental approach for gathering structural data on biomolecules.

It appears that there are several cross-peaks in the set of 2D spectra that cannot be associated with intramolecular correlations. For instance, carbon 2 appears to correlate with carbon 14, carbon 13^1 has a correlation with carbon 20, and carbon 4 has a correlation with carbon 12. The carbon atoms 12, 13^1 and 14 are on the opposite side of the Chl **a** ring with respect to carbons 2, 4 and 20. It is unlikely that these correlations are due to relayed intramolecular transfer. In that case cross-peaks with relaying carbons should also have been observed. Such cross-peaks are therefore most likely associated with short intermolecular distances. This indicates that the stacking of the Chl **a** rings proceeds roughly in agreement with the model of Chow et al. [17], which was based on the X-ray structure of ethyl chlorophyllide **a**, although the presence of the correlation between 13^1 and 20 suggests that the rings are rotated slightly along an axis perpendicular to the plane of the molecule, generating a curvature of the array of stacked rings which could explain the formation of tubular micelles in the Chl **a**/water aggregates. It is thus concluded that the experiment of Fig. 2 will help to pave the way for structure determination of uniformly enriched solids at the atomic level.

3. Experimental

Uniformly ^{13}C enriched Chl a was isolated from a cell culture of *Chenopodium rubrum*. Micelles of the highly enriched chlorophyll (13.7 mg, > 95% ^{13}C) were prepared according to the procedures described in Ref. [1] except that the hydration of the chlorophyll oligomers was performed in *n*-heptane.

For all NMR experiments a commercial MSL400 spectrometer (Bruker) equipped with a double resonance 4 mm CP/MAS probe was used. Spectra were collected with sweep widths between 30 and 50 kHz at various spinning speeds $7 < \omega_r/2\pi < 11$ kHz. The cycle time between scans was typically 1 s and data were acquired under continuous-wave ^{1}H heteronuclear dipolar decoupling with a ^{1}H nutation frequency of 60 kHz.

1D CP/MAS spectra were collected with a contact time of 4 ms at a $^{13}C-^{1}H$ Hartmann–Hahn matching condition [22]. For the 2D ^{13}C dipolar correlation spectroscopy experiments variable amplitude cross-polarisation (VACP) with a contact time of 2 ms was used [23]. During the VACP contact time the ^{1}H power level was varied between 35% and 65% of the cw decoupling power according to Fig. 2. Prior to the 2D correlation experiment, the VACP was optimized by adjusting the ^{13}C power for maximum signal intensity from a sample of glycine ^{13}C labelled at the quaternary carboxyl carbon. 32 dummy scans were used to saturate the initial thermal ^{13}C polarization. Subsequently, the 2D dataset was acquired in one experiment (buffered acquisition).

Calibration of the chemical shift was achieved by setting the chemical shifts for the two methyls P18 and P19 at the end of the phytyl chain at 20.0 ppm (cf. Fig. 1), the same value as in solution [15]. This is reasonable, as it is expected that the end of the tail of Chl a is quite mobile and not affected much by the aggregation. With this assumption the shifts of all carbons of the saturated tail of the phytyl chain (P4–P16, P18–P20) match the values in solution within 0.3 ppm.

The 2D data were analyzed using the NMR2 software (Tripos Associates). In the t_1 dimension a sine-square apodization, shifted by $\pi/2$, was used prior to Fourier transformation. In the t_2 dimension the resolution was enhanced with a Lorentz–Gauss

transformation. The correlations were extracted from the 2D data sets using the tools for the location of cross-peaks included in the analysis software.

Acknowledgement

References

[1] J.J. Katz, M.K. Bowman, T.J. Michalski and D.L. Worcester, in: Chlorophylls, ed. H. Scheer (CRC Press, Boca Raton, 1991) p. 211.

[2] H.C. Chow, R. Serlin and C.E. Strouse, J. Am. Chem. Soc. 97 (1975) 7230.

[3] R. Kaptein, R. Boelens, R.M. Scheek and W.F. van Gunsteren, Biochemistry 27 (1988) 5389;

[4] K. Wüthrich, Science 243 (1989) 45.

[5] A.E. Bennett, J.H. Ok, R.G. Griffin and S. Vega, J. Chem. Phys. 96 (1992) 8624.

[6] T. Gullion and S. Vega, Chem. Phys. Letters 194 (1992) 423.

[7] J.H. Ok, R.G.S. Spencer, A.E. Bennett and R.G. Griffin, J. Chem. Phys. Letters 197 (1992) 389.

[8] T. Gullion, D.B. Baker and S. Conradi, J. Magn. Reson. 89 (1990) 479.

[9] D.K. Sodickson, M.H. Levitt, S. Vega and R.G. Griffin, J. Chem. Phys. 98 (1993) 6742.

[10] O. Weintraub, S. Vega, Ch. Hoelger and H.H. Limbach, J. Magn. Reson. 109A (1994) 14.

[11] D. Marion and K. Wüthrich, Biochem. Biophys. Res. Com. 113 (1983) 967.

[12] A. Wokaun and R.R. Ernst, Chem. Phys. Letters 52 (1977) 407.

[13] C.E. Brown, R.B. Spencer, V.T. Burger and J.J. Katz, Proc. Nat. Acad. Sci. US 81 (1984) 641.

[14] S. Macura, Y. Huang, D. Suter and R.R. Ernst, J. Magn. Reson. 43 (1981) 259.

[15] R.J. Abraham and A.E. Rowan, in: Chlorophylls, ed. H. Scheer (CRC Press, Boca Raton, 1991) p. 797.

[16] C. Giessner-Prettre and B. Pullman, J. Theoret. Biol. 31 (1971) 287.

[17] H.-C. Chow, R. Serlin and C.E. Strouse, J. Am. Chem. Soc. 97 (1975) 7230.

[18] H. Strub, A.J. Beeler, D.M. Grant, J. Michl, P.W. Cutts and K. Zilm, J. Am. Chem. Soc. 105 (1983) 3333.

[19] F. Creuzet, A. McDermott, R. Gebhard, K. van der Hoef, M.B. Spijker-Assink, J. Herzfeld, Lugtenburg, M.H. Levitt and R.G. Griffin, Science 251 (1991) 783.

[20] J.M. Griffiths, K.V. Lakshmi, A.E. Bennett, J. Raap, C.M. van der Wielen, J. Lugtenburg, J. Herzfeld and R.G. Griffin, J. Am. Chem. Soc. 116 (1994) 10178.

[21] S.M. Holl, G.R. Marshall, D.D. Beusen, K. Kociolek, A.R. Redlinski, M.T. Leplawy, R.A. McKay, S. Vega and J. Schaefer, J. Am. Chem. Soc. 114 (1992) 4830.

[22] A. Pines, M.G. Gibby and J.S. Waugh, J. Chem. Phys. 59 (1973) 569.

[23] O.B. Peersen, X. Wu, I. Kustanuvich and S.O. Smith, J. Magn. Reson. 102A (1993) 1.